Modern Physics Letters B
Vol. 28, No. 24 (2014) 1450189 (12 pages)
© World Scientific Publishing Company
DOI: 10.1142/S0217984914501899

World Scientific
www.worldscientific.com

High fidelity quantum teleportation assistance with quantum neural network

Chunhui Huang* and Bichun Wu

College of Physics and Information Engineers, Fuzhou University, Fuzhou 350116, China
**hchuang@fzu.edu.cn*

Received 17 March 2014
Revised 9 June 2014
Accepted 13 August 2014
Published 19 September 2014

In this paper, a high fidelity scheme of quantum teleportation based on quantum neural network (QNN) is proposed. The QNN is composed of multi-bit control-not gates. The quantum teleportation of a qubit state via two-qubit entangled channels is investigated by solving the master equation in Lindblad operators with a noisy environment. To ensure the security of quantum teleportation, the indirect training of QNN is employed. Only 10% of teleported information is extracted for the training of QNN parameters. Then the outputs are corrected by the other QNN at Bob's side. We build a random series of numbers ranged in $[0, \pi]$ as inputs and simulate the properties of our teleportation scheme. The results show that the fidelity of quantum teleportation system is significantly improved to approach 1 by the error-correction of QNN. It illustrates that the distortion can be eliminated perfectly and the high fidelity of quantum teleportation could be implemented.

Keywords: QNN; error-correction; quantum teleportation; Lindblad; fidelity.

PACS Number(s): 0367.Pp, 03.67.HK, 03.67.Dd

Mod. Phys. Lett. B 2014.28. Downloaded from www.worldscientific.com
by UNIVERSITY OF CINCINNATI on 11/14/14. For personal use only.

1. Introduction

Quantum teleportation (QT), proposed by Bennett *et al.*,[1] is one of the most important transmission protocols in quantum information. As a promising communication method, it has attracted much attention in the last 20 years.[2–10] Prakash and Maurya[5] adopted the 3-qubit entangled states and the "magic bases" to transfer the quantum information. Adhikari *et al.*[6] proposed the method of QT based on non-orthogonal entangled channels. Man *et al.*[7,8] studied QT in a dissipative environment. Ma *et al.*[9,10] performed the experiment of QT over a high-loss free-space channel. Although QT has become one of the principal methods of quantum communication and achieved remarkable progress both in theoretical and experimental studies, there are still some obstacles in practice. For example, the decoherence will reduce the robustness of quantum-information transmission.[11]

Mod. Phys. Lett. B 2014.28. Downloaded from www.worldscientific.com
by UNIVERSITY OF CINCINNATI on 11/14/14. For personal use only.

In a practical quantum system, the quantum states will inevitably interact with the environment and gradually lose their coherence. Therefore, how to reduce the influence of noisy environment is very necessary in the quantum information processes and becomes as an important branch of study.[12–18] Jung *et al.*[15] analyzed the effects of noises on the process of QT via the noisy GHZ and W channels, and discussed the capacity of quantum channel against the influence of noisy environment. Hao *et al.*[16] investigated the effects of amplitude damping in quantum noise channels. They found that the non-maximally entangled channels were immune to quantum noise of teleportation to some degree. Hu *et al.*[17] studied the noise effect on the fidelity of two-qubit teleportation and considered that the inseparable channels never have the higher teleportation fidelity than Bell pairs even in the presence of collective noise. To improve the fidelity of teleportation, Pramanik and Majumdar[18] investigated the teleportation through two-qubit noisy channels using the weak measurement, the result showed that the fidelity could be improved in a certain range of decoherence.

Despite the apparent success of current studies, they all suffer from one major defect: The teleportation fidelity is limited and the highest fidelity measured with nowadays technology is close to 1 when only one particle of the two-qubit channel interacts with the environment by the weak measurement. Moreover, it is difficult to approach 1 in practice by optimizing the quantum channels or measurement methods.

In order to enhance the quality of teleportation, we propose a novel error-correction scheme for the teleportation of a qubit state, so that the fidelity can easily approach 1. Instead of using the weak measure technique and the optimization in quantum channels, we use QNN algorithm to correct outputs of QT. For communication security, we apply an indirect training of QNN to correct the errors. Only 10% of teleported information at Alice's side is extracted to train the weight parameters of QNN, then the trained parameters are used to correct the outputs by another QNN at Bob's side. In our scheme, the QNN is composed of multi-bit controlled-not (CNOT) gates. The quantum channel is estimated by solving the master equation of Lindblad operators, so that the errors of outputs affected by the ambient noise can be analytically deduced and the noise channel can be built to simulate the noise environment. By high precision training ability of QNN, the error-correction almost eliminates the distortion and makes the fidelity approach 1. Although only the Pauli noises are considered in quantum communication system (QCS), we consider that the scheme can be applied to other noises because of the strong learning ability and adaptability of QNN.

2. Teleporting a Qubit State in Noisy Environments

QT is a typical representative of QCS where Alice and Bob share a bipartite EPR state. As shown in Fig. 1, the original signal is divided into two parts: One is

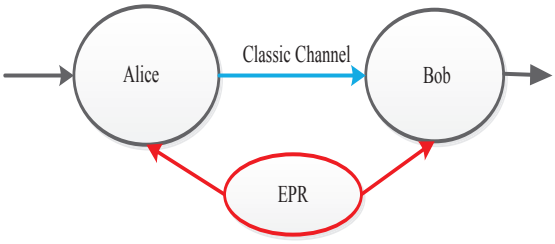

Fig. 1. (Color online) The QT system consists of Alice, Bob and ERP state. The *blue line* — the classic channel. The *red lines* — quantum channel.

Mod. Phys. Lett. B 2014.28. Downloaded from www.worldscientific.com
by UNIVERSITY OF CINCINNATI on 11/14/14. For personal use only.

transmitted in classic channels as the *blue lines*, the other is transmitted in quantum channel as the *red lines* from the Alice to Bob.[15–21]

Ideally, quantum states non-interact with the external environment, the single-qubit state teleported from Alice to Bob is described as follows:

$$|\psi\rangle_1 = \cos(\theta/2)|0\rangle_1 + \sin(\theta/2)e^{i\zeta}|1\rangle_1\,, \tag{1}$$

where $\theta \in [0, \pi]$ and $\zeta \in [0, 2\pi)$ are the polar and azimuthal angles of the teleported state, respectively. A pure entangled state $|\psi\rangle_{23} = a|00\rangle_{23} + b|11\rangle_{23}$ is shared by Alice and Bob, where the constants a and b satisfy $|b| \leq |a|$, $|a|^2 + |b|^2 = 1$. Alice possesses particle 2 and Bob particle 3. The state $|\psi\rangle_{23}$ can be transformed into the maximally entangled EPR state by adding an auxiliary qubit with the original state $|0\rangle_4$ at Bob, as shown in Fig. 2.[22,23] The *1st line* is the initial state to be teleported by Alice, the *2nd line* is the state of first particle of EPR channel belonging to Alice, the *3rd line* represents the state of the second particle of the EPR channel belonging to Bob, and the *4th line* represents the state of the auxiliary particle. The total state of the particles 2, 3 and 4 is $|\psi\rangle_{234} = |\psi\rangle_{23} \otimes |0\rangle_4 = a|000\rangle_{234} + b|110\rangle_{234}$. If Bob performs a unitary transformation U_{34} on particles 3 and 4 of $|\psi\rangle_{234}$ as follows:

$$U_{34}|\psi\rangle_{234} = b(|00\rangle_{23} + |11\rangle_{23})|0\rangle_4 + \sqrt{a^2 - b^2}\,|00\rangle_{23}|1\rangle_4\,, \tag{2}$$

where $U_{34} = ((b/a)|00\rangle\langle 00| - \sqrt{1 - b^2/a^2}\,|00\rangle\langle 01| + \sqrt{1 - b^2/a^2}\,|01\rangle\langle 00| + (b/a)|01\rangle\langle 01| + |10\rangle\langle 10| + |11\rangle\langle 11|)$.[24] Bob can obtain $|\psi\rangle_{23} = (|00\rangle_{23} + |11\rangle_{23})/2$ state successfully with probability of $2|b|^2$, when $|0\rangle_4$ state is measured. It means that the $|\psi\rangle_1$ can be teleported from Alice to Bob via the maximally entangled EPR state $|\psi\rangle_{23}$ following the procedure of the standard QT protocol stated in Ref. 24. Otherwise Bob obtains $|1\rangle_4$ with probability of $a^2 - b^2$, the teleportation is failure.

In a practical QCS, the quantum states will inevitably interact with the environment. Pauli noises are the basic errors of Markovian noises, including the bit flip, the dephasing, the bit-phase flip, and so on.[25,26] As the approximations of Markov and Born, the dynamics of an open quantum system can be described by the following master equation of Lindblad operators:

$$\frac{\partial \rho}{\partial t} = -\frac{i}{\hbar}[H, \rho] + \sum_{j,\alpha}\left(L_{j,\alpha}\rho L_{j,\alpha}^{\dagger} - \frac{1}{2}L_{j,\alpha}^{\dagger}L_{j,\alpha}\rho - \frac{1}{2}\rho L_{j,\alpha}^{\dagger}L_{j,\alpha}\right), \tag{3}$$

where H is Hamiltonian of the quantum system. The Lindblad operator $L_{j,\alpha} = \sqrt{k_{j,\alpha}}\sigma_\alpha^j$ represents the coupling of the system and environment, σ_α^j $(\alpha = x, y, z)$ denotes the Pauli operator of the jth qubit and $k_{j,\alpha}$ is the jth qubit's spontaneous emission rate. According to Eq. (3), the time evolution of the teleported state $|\psi\rangle_1$ and the EPR state $|\psi\rangle_{23}$ are analytically resolved. Let the noise only affects the quantum channel, Lindblad operators acting on $|\psi\rangle_{23}$ can be taken as follows:

$$L_{2,x} = L_{3,x} = \sqrt{k_1}\sigma_x, \quad L_{2,y} = L_{3,y} = \sqrt{k_2}\sigma_y, \quad L_{2,z} = L_{3,z} = \sqrt{k_3}\sigma_z\,, \tag{4}$$

where $k_i = (k_i)_{2,\alpha} = (k_i)_{3,\alpha}$ $(i = 1, 2, 3)$. In this paper, $[H, \rho] = 0$, i.e. H commutes with ρ. According to (3), (4) and $|\psi\rangle_{23}$, the density matrix of the time state, ρ_{23}^{evo} can be derived as follows:

$$\rho_{23}^{\text{evo}} = \begin{pmatrix} \rho_{23}^{11} & \rho_{23}^{12} & \rho_{23}^{13} & \rho_{23}^{14} \\ \rho_{23}^{21} & \rho_{23}^{22} & \rho_{23}^{23} & \rho_{23}^{24} \\ \rho_{23}^{31} & \rho_{23}^{32} & \rho_{23}^{33} & \rho_{23}^{34} \\ \rho_{23}^{41} & \rho_{23}^{42} & \rho_{23}^{43} & \rho_{23}^{44} \end{pmatrix}, \tag{5}$$

where superscripts represent the indexes of matrix elements, subscripts represent particles 2 and 3. The elements are as follows:

$$\rho_{23}^{11} = \frac{1}{4}[1 + 2(a^2 - b^2)e^{-2(k_1+k_2)t} + e^{-4(k_1+k_2)t}], \quad \rho_{23}^{22} = \frac{1}{4}[1 - e^{-4(k_1+k_2)t}],$$

$$\rho_{23}^{33} = \frac{1}{4}[1 - e^{-4(k_1+k_2)t}], \quad \rho_{23}^{44} = \frac{1}{4}[1 - 2(a^2 - b^2)e^{-2(k_1+k_2)t} + e^{-4(k_1+k_2)t}],$$

$$\rho_{23}^{14} = \rho_{23}^{41} = \frac{1}{2}ab[e^{-4(k_1+k_3)t} + e^{-4(k_2+k_3)t}]\,,$$

$$\rho_{23}^{23} = \rho_{23}^{32} = \frac{1}{2}ab[-e^{-4(k_1+k_3)t} + e^{-4(k_2+k_2)t}]\,,$$

$$\rho_{23}^{12} = \rho_{23}^{13} = \rho_{23}^{21} = \rho_{23}^{24} = \rho_{23}^{31} = \rho_{23}^{34} = \rho_{23}^{42} = \rho_{23}^{43} = 0\,.$$

As shown in Fig. 2, *the dash box* represents the dephasing noise acting on the quantum channel. In this situation, the output at Bob can be expressed as

$$\rho_{\text{out}} = \text{Tr}_{1,2}\{U_{\text{tel}}(|\psi\rangle_1\langle\psi| \otimes \rho'_{23})U_{\text{tel}}^\dagger\}\,, \tag{6}$$

where $U_{\text{tel}} = (\sigma_z)_{1\to3}(\sigma_x)_{2\to3}H_1(\text{CNOT})_{1\to2}$, $\text{CNOT} = |0\rangle\langle0| \otimes I + |1\rangle\langle1| \otimes \sigma_x$. $\rho'_{23} = \text{Tr}_4\{M[I_2 \otimes U_{34}(\rho_{23}^{\text{evo}} \otimes |0\rangle_4\langle0|)(I_2 \otimes U_{34})^\dagger]M^\dagger\}$. H_1 is the Hadamard operation. $M = |0\rangle_4\langle0|$ is a projection operator on particle 4. $(\sigma_w)_{u\to v}$ is a two-qubit controlled-σ_w $(w = x, z)$ gate with particle u controlling particle v $(u = 1, 2$ and $v = 2, 3)$. If quantum channel is only infected by the dephasing noise, i.e. $k_1 = k_2 = 0$, $k_3 = k$, the matrix elements of ρ_{23}^{evo} under the action of dephasing noise are $\rho_{23}^{11} = a^2$, $\rho_{23}^{44} = b^2$, $\rho_{23}^{14} = \rho_{23}^{41} = ab \cdot e^{-4kt}$ and $\rho_{23}^{22} = \rho_{23}^{33} = \rho_{23}^{23} = \rho_{23}^{32} = 0$. So $\rho'_{23} = 1/2(|00\rangle\langle00| + e^{-4kt}|00\rangle\langle11| + e^{-4kt}|11\rangle\langle00| + |11\rangle\langle11|)$.

The distortion quality is described by the fidelity.[27,28] It is written as follows:

$$F \equiv \langle\psi_1|\rho_{\text{out}}|\psi_1\rangle\,. \tag{7}$$

Mod. Phys. Lett. B 2014.28. Downloaded from www.worldscientific.com by UNIVERSITY OF CINCINNATI on 11/14/14. For personal use only.

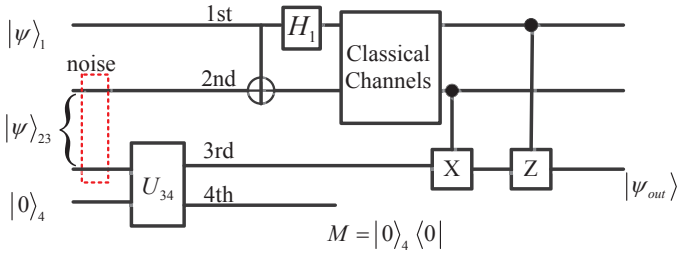

Fig. 2. (Color online) The quantum circuit for the teleportation a qubit state $|\psi\rangle_1$ with the influence of noise. The *dash box* — the noise acting on the quantum channel.

Mod. Phys. Lett. B 2014.28. Downloaded from www.worldscientific.com
by UNIVERSITY OF CINCINNATI on 11/14/14. For personal use only.

3. The Error-Correction Based on QNN in QT System

This section describes how to eliminate the distortion by QNN. QNN as a novel computing paradigm is combined the artificial neural network with quantum computing, which has many advantages based on the algorithm of quantum associative memory and the general quantum logic gates, such as a large storage capacity of information, high fault-tolerance, well adaptability, powerful error-correcting ability, and so on.[29–35] Here the QNN performs a post-processing similar to the reconciliation proceeding in single-photon QKD.

3.1. *The structure of QNN*

The QNN model consisting of input-layer, hidden-layer and output-layer is shown in Fig. 4. The inputs, $|P\rangle = (|p_1\rangle|p_2\rangle\cdots|p_n\rangle)^T$, are corresponding to the quantum states $|X\rangle = (|x_1\rangle|x_2\rangle\cdots|x_n\rangle)^T \cdot |h_1\rangle, |h_2\rangle, \ldots, |h_p\rangle$ and $|y_1\rangle, |y_2\rangle, \ldots, |y_m\rangle$ are the outputs of hidden-layer and output-layer, respectively. U transforms the quantum state into classical information. The quantum rotation gates $\tau(\vartheta)$ and $\tau(\varphi)$ are the weights of QNN, where

$$\tau(\vartheta) = \begin{pmatrix} \tau(\vartheta_{11}) & \cdots & \tau(\vartheta_{q1}) \\ \vdots & & \vdots \\ \tau(\vartheta_{1n}) & \cdots & \tau(\vartheta_{qn}) \end{pmatrix}, \text{ where } \tau(\vartheta_{ji}) = \begin{pmatrix} \cos\vartheta_{ji} & -\sin\vartheta_{ji} \\ \sin\vartheta_{ji} & \cos\vartheta_{ji} \end{pmatrix},$$

$$i = 1, 2, \ldots, n; j = 1, 2, \ldots, p,$$

$$\tau(\varphi) = \begin{pmatrix} \tau(\varphi_{11}) & \cdots & \tau(\varphi_{m1}) \\ \vdots & & \vdots \\ \tau(\varphi_{1q}) & \cdots & \tau(\varphi_{mq}) \end{pmatrix}, \text{ where } \tau(\varphi_{kj}) = \begin{pmatrix} \cos\varphi_{kj} & -\sin\varphi_{kj} \\ \sin\varphi_{kj} & \cos\varphi_{kj} \end{pmatrix},$$

$$k = 1, 2, \ldots, m; j = 1, 2, \ldots, p.$$

In Fig. 3, the inputs are $|x_i\rangle = \cos t_i|0\rangle + \sin t_i|1\rangle$, $i = 1, 2, \ldots, n$. According to the structure of QNN in Figs. 3 and 4, the outputs of hidden-layer are

Mod. Phys. Lett. B 2014.28. Downloaded from www.worldscientific.com
by UNIVERSITY OF CINCINNATI on 11/14/14. For personal use only.

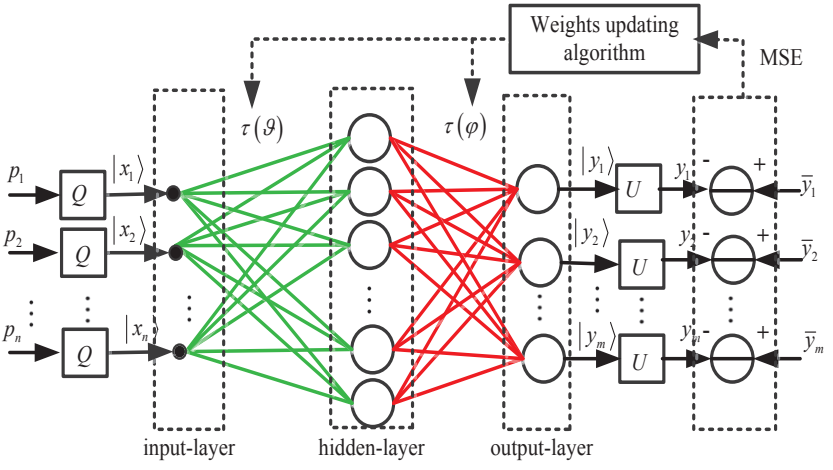

Fig. 3. (Color online) The model of QNN. The *green lines* — the weights connecting input-layer with hidden-layer. The *red lines* — the weights connecting hidden-layer with output-layer. The circles — the neurons.

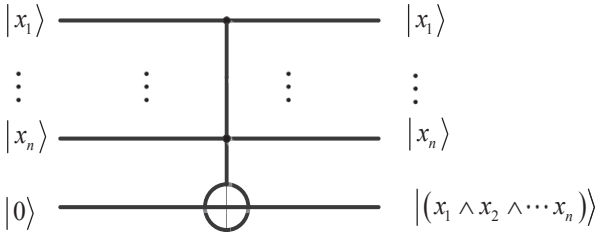

Fig. 4. The model of neuron which is CNOT gate.

$|h_j\rangle = |0\rangle \prod_{i=1}^{n} \cos(t_i + \vartheta_{ij}) + |1\rangle \prod_{i=1}^{n} \sin(t_i + \vartheta_{ij})$, $j = 1, 2, \ldots, p$ and outputs of QNN are $|y_k\rangle = |0\rangle \prod_{i=1}^{p} \cos(v_i + \varphi_{ij}) + |1\rangle \prod_{i=1}^{p} \sin(v_i + \varphi_{ij})$, $k = 1, 2, \ldots, m$ where $v_i = \arcsin(\prod_{i=1}^{n} \sin(t_i + \vartheta_{ij}))$.

Assuming the probability of $|1\rangle$ from quantum neurons is a real output. After the $U = \left(\begin{smallmatrix} 0 & 0 \\ 0 & 1 \end{smallmatrix}\right)$ operate, the outputs of hidden-layer and output-layer can be expressed as

$$h_j = U|h_j\rangle = \sin(\varphi_j) = \prod_{i=1}^{n} \sin(t_i + \vartheta_{ij}), \tag{8}$$

$$y_k = U|y_k\rangle \prod_{j=1}^{p} \sin(\varphi_j + \varphi_{jk}) = \prod_{j=1}^{p} \left(\sin \left(\arcsin \prod_{i=1}^{n} \sin(t_i + \vartheta_{ij}) \right) + \varphi_{jk} \right). \tag{9}$$

The expectations of QNN are $\bar{y}_k = \sin t_k, k = 1, 2, \ldots, m$. The mean square error (MSE) is MSE $= 1/2 \sum_{k=1}^{m} (\bar{y}_k - y_k)^2$. By the gradient descent method, the

phase rotation training formulas of each layer are

$$\vartheta_{ij}(n+1) = \vartheta_{ij}(n) + \eta\Delta_\theta, \quad \varphi_{jk}(n+1) = \varphi_{jk}(n) + \eta\Delta_\varphi\,, \tag{10}$$

where

$$\Delta_\theta = -\frac{\partial \mathrm{MSE}}{\partial \vartheta_{ij}} = \cot(\varphi_j + \varphi_{jk}) h_j \cot(t_i + \vartheta_{ij}) \sum_k^m \delta_k \sqrt{1 - h_j^2}\,,$$

$$\delta_k = (\bar{y}_k - y_k) y_k, \quad \Delta_\varphi = -\frac{\partial \mathrm{MSE}}{\partial \varphi_{jk}} = (\bar{y}_k - y_k) y_k \cot(\varphi_j + \varphi_{jk})\,,$$

n is the number of iterations and η is the learning rate.

3.2. *The error-correction by QNN*

Ideally, if QT teleports an unknown quantum state, the transmission is secure. In a noisy environment, the quantum states will interact with the noise that causes the distortion of quantum information. Therefore, a post process of error-correction is necessary to eliminate the distortion and improve the teleportation fidelity. We propose a scheme of error-correction with QNN. In this scheme, an indirect QNN structure is introduced in QCS as Fig. 5, which includes two QNNs, one called *distortion simulator* is used to train the parameters of QNN; The other called *error-corrector* is applied to correct the outputs of QCS with parameters of *distortion simulator*. For security reason, only 10% of information is extracted as expectations. The *distortion simulator* trains the QNN's parameters with the guidance of expectation, and copies the trained parameters to the *error-corrector* as the weights of QNN. Then the *error-corrector* corrects the outputs. This proceeding maintains the security of QT.

Figure 5 is the error-correction scheme of QT based on the QNN. The inputs $\{S_q, q = 1, 2, \ldots, N\}$ are the polar angles. The *block Q* performs a transformation from the classic information into the quantum states.

The steps of error-correction are as follows:

Step 1. Let $\zeta = 0$, Eq. (1) becomes $|\psi\rangle = \cos(\theta/2)|0\rangle + \sin(\theta/2)|1\rangle$. The samples are quantized as $|X_q\rangle = \cos(S_q/2)|0\rangle + \sin(S_q/2)|1\rangle$.

Step 2. Bob gets the outputs. The initial state $|X_q\rangle$ is teleported in QT. If Bob gets $|0\rangle_4$ from *4th line*, the qubit state $|X_q\rangle$ would be teleported successfully by means of a dephasing noise EPR state as Fig. 2. The mixed density outputs $(\rho_{\mathrm{out}})_q$ are obtained based on Eq. (5).

Step 3. Get the amplitude of $|i_0\rangle, i_0 = 0$ or 1. The pure state $|X_q\rangle$ distorts through the noise channel, namely, the amplitudes of $|i_0\rangle$ have been changed. We recover the amplitude value of $|i_0\rangle$ and reconstruct the pure state as $|\psi\rangle$ according to the normalization. So the amplitude value $(b_0)_q$ can be obtained by $\langle i_0|(\rho_{\mathrm{out}})_q|i_0\rangle$.

Mod. Phys. Lett. B 2014.28. Downloaded from www.worldscientific.com
by UNIVERSITY OF CINCINNATI on 11/14/14. For personal use only.

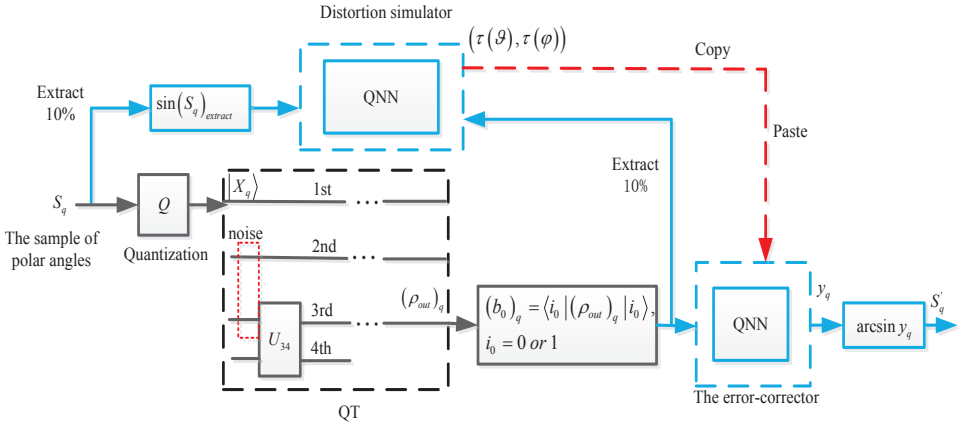

Fig. 5. (Color online) The error-correction scheme of QT based on the QNN. S_i — the samples. Q — the transformation from the classic information into the quantum states. S_i' — the outputs after the correction of QNN.

Step 4. The weight parameters of error-corrector are trained in distortion simulator. This simulator consists of 1 neuron in input-layer, 10 in hidden-layer and 1 in output-layer, namely, $n = 1, p = 10, m = 1$. When S_q is sent and Bob gets $(b_0)_q$ at one moment, $\{(b_0)_{q'}, q' = 1, 2, \ldots, N/10\}$ are extracted randomly by distortion simulator as the inputs and the corresponding $\{S_{q'}, q' = 1, 2, \ldots, N/10\}$ are extracted as the expectations. The weight parameters of QNN can be obtained by the training of distortion simulator according to the Eqs. (8)–(10).

Step 5. The error-corrector corrects $\{(b_0)_{q''}, q'' = 1, 2 \ldots, 9N/10\}$, making use of the weight parameters trained in distortion simulator. The structure of error-corrector is similar to distortion simulator without the training parameters. According to Eq. (9), the results of correction can be described as

$$y_{q''} = \prod_{j=1}^{10} \sin(\varphi_j + \varphi_{j1}) = \prod_{j=1}^{10} \sin(\arcsin(\sin(t_{q''} + \vartheta_{i1})) + \varphi_{j1}), \qquad (11)$$

where $t_{q''} = 2\pi/(1 + e^{-(b_0)_{q''}})$, $q'' = 1, 2, \ldots, 9N/10$.

Step 6. The outputs can be recovered by $S'_{q''} = \arcsin y_{q''}$, $q'' = 1, 2, \ldots, 9N/10$.

4. Simulation and Discussion

The QT system with the error-correction of QNN is shown as Fig. 5. We simulate the error-correction of QNN with $\{S_q, q = 1, 2, \ldots, 10000, 0 \leq S_q \leq \pi\}$, $k_1 = k_2 = 0$, $k_3 = 0.5$, $n = 1, p = 10, m = 1$, $\eta = 0.25$, MSE $\leq 1 \times 10^{-6}$. Noting that F is not affected by ζ in Eq. (6), let $\zeta = 0$ in Step 1 of Sec. 3. The result show that the fidelity F decays continuously to the stable values with the evolution of time, as shown in Fig. 6.

Mod. Phys. Lett. B 2014.28. Downloaded from www.worldscientific.com
by UNIVERSITY OF CINCINNATI on 11/14/14. For personal use only.

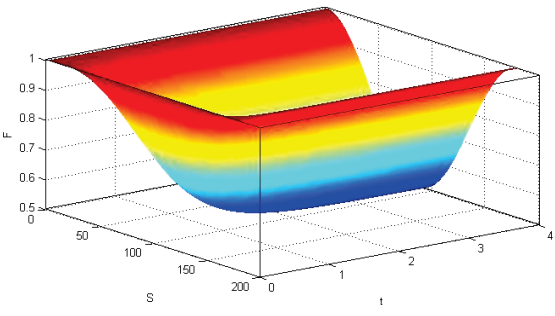

Fig. 6. (Color online) The relationship between the fidelity F and θ, t under the dephasing noise without the error-correction of QNN where $k_3 = 0.5$ and $a = b = \sqrt{2}/2$.

Mod. Phys. Lett. B 2014.28. Downloaded from www.worldscientific.com
by UNIVERSITY OF CINCINNATI on 11/14/14. For personal use only.

It is easy to see that the influence of noisy channel changes with the evolution of time and distortion of QT changes with the different θs of initial states. Bob's information is subjected to the distortion in different degrees for different inputs and evolution time. It means that the teleportation is failure between Alice and Bob.

In this paper, Alice sends $\{S_q, q = 1, 2, \ldots, 10000\}$ and Bob gets $(\rho_{\text{out}})_q$, when $t = 1$. The fidelity F is in the range of $0.57 \leq F \leq 1$ for the random angles in $[0, \pi]$, as shown in Fig. 7(a). However, the error-correction of QNN is able to enhance the teleportation fidelity close to 1 for most random angles, as shown in Fig. 7(b). The results hold perfectly for all maximally entangled channels, as well as for all original inputs. It means that Bob will receive almost consistent information with Alice in QCS.

In the process of correction, $(b_0)_q$ are divided into 10 slices. Each slice has 1000 datum. In every slice, the first 100 datum are extracted by distortion simulator to train the weight parameters which will be copied to the error-corrector and the remaining 900 datum are corrected directly by error-corrector. Moreover, the next slice parameters updates on the basis of this slice, so that the correction precision improves constantly. As shown in Fig. 7(b), the first 900 fidelities have more dots less than 1, compared with the next 900 fidelities. The fidelities tend to stable until the forth slice. The mean fidelity is larger than 0.9 and almost all dots approach 1.

The QNN in our scheme has a superior property of convergence as shown in Fig. 8. The variables are changing as Eq. (10) until the MSE is lower than 1×10^{-6}. The numerical simulation demonstrates that the QNN not only has a fast convergence performance, but also has high a precision. MSE quickly achieves a stable value close to 9.3889×10^{-6} by 55 iterations. We have verified that the convergence performance of classical neural network (NN) is lower than QNN. The MSE is only about 0.006 after 55 iterations by the NN. The fidelities by the correction of NN are in the range of $0.83 < F \leq 1$ after 1000 iterations. And most of dots are only above 0.96. So we believe that the learning and generalization ability of QNN is stronger than the NN.

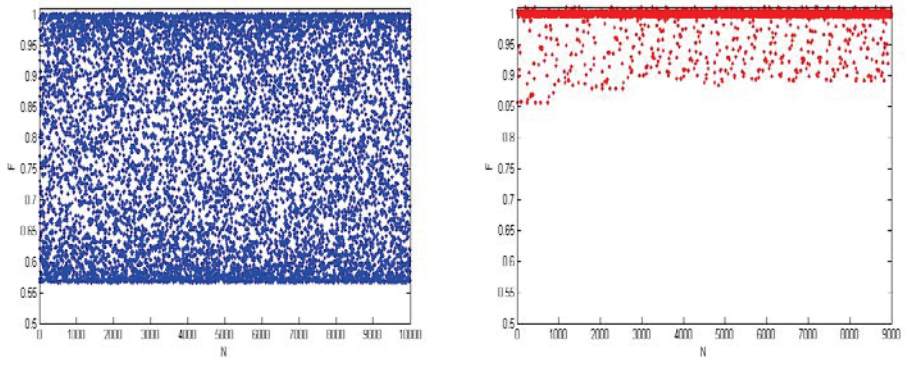

(a) (b)

Fig. 7. (Color online) The scattergrams of F under the dephasing noise where $k_3 = 0.5$, $t = 1$ and $a = b = \sqrt{2}/2$. (a) Without the error-correction of QNN. (b) With the error-correction of QNN.

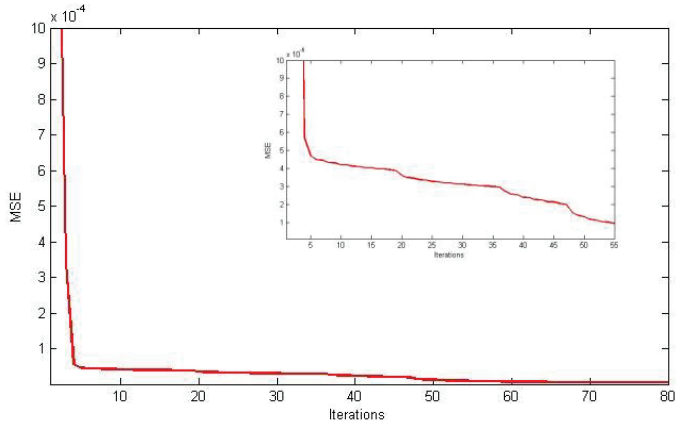

Fig. 8. (Color online) The convergence curve of MSE where $n = 1p = 10$, $m = 1$, $\eta = 0.25$ and $(\text{MSE})_{\min} = 1 \times 10^{-6}$.

For the interaction between EPR states and environment noise, our scheme reduces the loss of information in the QCS, and enhance the fidelity close to 1 as shown in Fig. 7(b). This result holds perfectly for all quantum channels of two-particle maximally entangled states. It is significantly better than the original fidelity in the range of $0.55 \leq F \leq 1$ shown as Fig. 6. To our knowledge, the highest fidelity measured with nowadays technology is close to 1 by using the optimal strength of reversing the measurement in Ref. 18 when only one particle interacts with environment. But in a practical QCS, both particles in quantum channels will inevitably interact with the environment, the quantum states gradually lose their coherence. The method of Ref. 18 cannot make the loss of information minimum. However, after the error-correction of QNN, the fidelity can easily approach 1 for most

Mod. Phys. Lett. B 2014.28. Downloaded from www.worldscientific.com
by UNIVERSITY OF CINCINNATI on 11/14/14. For personal use only.

teleported information in the noise environment. We can achieve the high-precision information transmission and the MSE downs to 9.3889×10^{-6} shown as Fig. 8. Because of the robustness of QNN, the QCS transmits the information more precisely and quickly than Ref. 18. In addition, compared with the existing scheme, the QNN is easier to realize with the current technology than the weak measure technique or the optimization in quantum channels.

5. Summary

In this paper, an error-correction scheme of QNN is proposed for an entangled channel with noise. By solving the master equation of Lindblad operators, the quantum channel in noisy environments is estimated. To ensure the security of QT, the indirect training of QNN is used to train the weight parameters and only a small fraction of information is extracted. The error-correction of QNN is applied to eliminate the information loss of unknown state produced by the dephasing noise channel. The results demonstrate that error-correction of QNN can enhance the fidelity of QCS close to 1 for almost all teleported information in the coupling channel of the maximally entangled states and environment. Due to the robustness of QNN, the QCS transfers the information more precisely than the existing scheme. Although only processing the Pauli noise in this, it is emphasized that the scheme can be applied to other noises since the strong learning ability and adaptability of QNN.

Mod. Phys. Lett. B 2014.28. Downloaded from www.worldscientific.com
by UNIVERSITY OF CINCINNATI on 11/14/14. For personal use only.

Acknowledgment

This paper was supported by the National Natural Science Foundation of China (Grant No. 61177072).

References

1. C. H. Bennett, G. Brassard, C. Crépeau, R. Jozsa, A. Peres and W. K. Wootters, *Phys. Rev. Lett.* **70** (1993) 1895.
2. I. Sándor, M. Paulo, N. Péter and Z. Anton, *IEEE Commun. Mag.* **51** (2013) 26–27.
3. K. Yang, L. S. Huang, W. Yang and S. Fang, *Int. J. Theor. Phys.* **48** (2009) 516–521.
4. P. Hari, *Int. Indian J. Phys.* **84**(8) (2010) 1021–1029.
5. H. Prakash and A. K. Maurya, *Opt. Commun.* **284**(20) (2011) 5024–5030.
6. S. Adhikari, A. S. Majumdar, D. Home, A. K. Pan and P. Joshi, *Phys. Scripta* **85**(4) (2012) 045001.
7. Z. X. Man and Y. J. Xia, *Quantum Inf. Process.* **11**(6) (2012) 1911–1920.
8. Ş. K. Özdemir, K. Şartkiewicz, Y. X. Liu and A. Miranowicz, *Phys. Rev. A* **76**(4) (2007) 042325.
9. X. S. Ma, S. Kropatschek, W. Naylor, T. Scheidl, J. Kofler, T. Herbst, A. Zeilinger and R. Ursin, *Opt. Express* **20**(21) (2012) 23126–23137.
10. X. M. Jin, J. G. Ren, B. Yang, Z. H. Yi, F. Zhou, X. F. Xu and J. W. Pan, *Nat. Photon.* **4**(6) (2010) 376–381.
11. M. Berta, M. Christandl, F. G. Brandao and S. Wehner, *IEEE Int. Symp. Information Theory Proc.* (*ISIT*) (2012), pp. 900–904.

12. P. Agrawal and A. Pati, *Phys. Rev. A* **74**(6) (2006) 062320.
13. E. Jung, M. R. Hwang, D. Park, J. W. Son and S. Tamaryan, *J. Phys. A: Math. Theor.* **41**(38) (2008) 385302.
14. J. L. Hsu, Y. T. Chen, C. W. Tsai and T. Hwang, *Int. J. Theor. Phys.* (2012) 1–6.
15. E. Jung, M. R. Hwang, Y. H. Ju, M. S. Kim, S. K. Yoo, H. Kim, D. K. Park, J. W. Son, S. Tamaryan and S. K. Cha, *Phys. Rev. A* **78**(1) (2008) 012312.
16. X. Hao, R. Zhang and S.-Q. Zhu, *Commun. Theor. Phys.* **45**(5) (2006) 802.
17. X. Hu, Y. Gu, Q. Gong and G. Guo, *Phys. Rev. A* **81**(5) (2010) 054302.
18. T. Pramanik and A. S. Majumdar, *Phys. Lett. A* **377**(44) (2013) 3209–3215.
19. Y. Z. Wang, *Stat. Sci.* **27**(3) (2012) 373–394.
20. E. Beltrametti, M. L. Dalla Chiara, R. Giuntini and G. Sergioli, *Math. Slovaca* **62**(6) (2012) 1121–1144.
21. M. Al-Amri, J. Evers and M. S. Zubairy, *Phys. Rev. A* **82**(2) (2010) 022329.
22. Y. H. Kim, S. P. Kulik and Y. Shih, *Phys. Rev. Lett.* **86**(7) (2001) 1370.
23. H. Q. Liang, J. M. Liu, S. S. Feng and J. G. Chen, *Quantum Inf. Process.* **12**(8) (2013) 2671–2687.
24. W. L. Li, C. F. Li and G.-C. Guo, *Phys. Rev. A* **61** (2000) 034301.
25. Y. Yeo, Z. W. Kho and L. Wang, *Europhys. Lett.* **86**(4) (2009) 40009.
26. K. Fujii, arXiv:0803.3105.
27. S. Oh, S. Lee and H. W. Lee, *Phys. Rev. A* **66**(2) (2002) 022316.
28. M. L. Hu, *Eur. Phys. J. D* **64**(2–3) (2011) 531–538.
29. E. C. Behrman, J. E. Steck, P. Kumar and K. A. Walsh, arXiv:0808.1558.
30. M. Panella and G. Martinelli, *Int. J. Circuit Theor. Appl.* **39**(1) (2011) 61–77.
31. A. A. Segher and N. Metwally, arXiv:0912.2512.
32. A. Narayanan and T. Menneer, *Inf. Sci.* **128**(3) (2000) 231–255.
33. E. C. Behrman and J. E. Steck, arXiv:1301.2808.
34. E. C. Behrman, R. E. F. Bonde, J. E. Steck and J. F. Behrman, arXiv:1301.6107.
35. D. Mu, Z. Guan and H. Zhang, *Int. J. Comput. Theor. Eng.* **5**(5) (2013).

Mod. Phys. Lett. B 2014.28. Downloaded from www.worldscientific.com
by UNIVERSITY OF CINCINNATI on 11/14/14. For personal use only.